Unconventional field-induced spin gap in an $S = 1/2$ chiral staggered chain

J. Liu,[1] S. Kittaka,[2] R. D. Johnson,[1] T. Lancaster,[3] J. Singleton,[4] T. Sakakibara,[2] Y. Kohama,[2] J. van Tol,[5] A. Ardavan,[1] B. H. Williams,[1] S. J. Blundell,[1] Z. E. Manson,[6] J. L. Manson,[6,*] and P. A. Goddard[7,†]

[1]*Department of Physics, Clarendon Laboratory, University of Oxford, Parks Road, Oxford OX1 3PU, UK*
[2]*Institute for Solid State Physics, University of Tokyo, Kashiwa, Chiba 277-8581, Japan*
[3]*Centre for Materials Physics, Durham University, South Road, Durham DH1 3LE, UK*
[4]*National High Magnetic Field Laboratory, Los Alamos National Laboratory, MS-E536, Los Alamos, NM 87545, USA*
[5]*National High Magnetic Field Laboratory, Florida State University, Tallahassee, Florida 32310, USA*
[6]*Department of Chemistry and Biochemistry, Eastern Washington University, Cheney, WA 99004, USA*
[7]*Department of Physics, University of Warwick, Gibbet Hill Road, Coventry, CV4 7AL, UK*

We investigate the low-temperature magnetic properties of the molecule-based chiral spin chain $[Cu(pym)(H_2O)_4]SiF_6{\cdot}H_2O$ (pym = pyrimidine). Electron-spin resonance, magnetometry and heat capacity measurements reveal the presence of staggered g tensors, a rich low-temperature excitation spectrum, a staggered susceptibility and a spin gap that opens on the application of a magnetic field. These phenomena are reminiscent of those previously observed in non-chiral staggered chains, which are explicable within the sine-Gordon quantum-field theory. In the present case, however, although the sine-Gordon model accounts well for the form of the temperature-dependence of the heat capacity, the size of the gap and its measured linear field dependence do not fit with the sine-Gordon theory as it stands. We propose that the differences arise due to additional terms in the Hamiltonian resulting from the chiral structure of $[Cu(pym)(H_2O)_4]SiF_6{\cdot}H_2O$, particularly a uniform Dzyaloshinskii-Moriya coupling and a four-fold periodic staggered field.

Quantum phase transitions can be driven between gapped and gapless phases by applied magnetic field. This was demonstrated in $S = 1$ quasi-one dimensional (Q1D) chains [1] and $S = 1/2$ two-leg ladders [2–4]. These systems possess a spin gap that is closed by an external field, leading to a transition to a gapless phase which can be described by the Tomonaga-Luttinger liquid (TLL) theory [5]. In contrast, the excitation spectrum of $S = 1/2$ antiferromagnetic (AF) Heisenberg chains with uniform nearest-neighbor interactions is gapless up to the saturation field. However, this ground state is highly sensitive to small modifications. The dramatic effect of alternating local spin environments was first discovered through high-field neutron scattering and heat capacity experiments on the $S = 1/2$ AF staggered chain, Cu-benzoate $[Cu(C_6D_5COO)_2{\cdot}3D_2O]$ [6]. Here, the presence of alternating g tensors as well as Dzyaloshinskii-Moriya (DM) interactions produce an internal staggered field perpendicular to the external field. The staggered field breaks rotational symmetry around the applied field, leading to a field-induced spin gap and anisotropic staggered susceptibility [7, 8]. This gapped phase can be described using the sine-Gordon (SG) quantum-field theory [8] and a complex excitation spectrum is predicted including solitons, antisolitons and soliton-antisoliton bound states called breathers [8–10]. Such excitations were experimentally confirmed by electron spin resonance (ESR) in the SG spin chain $[pym\text{-}Cu(NO_3)_2(H_2O)_2]$ (pym = pyrimidine) [11, 12]. So far these studies have been limited to g tensors that alternate with a two-fold periodicity along the chain.

In this letter, we report a detailed investigation of the chiral chain $[Cu(pym)(H_2O)_4]SiF_6{\cdot}H_2O$, in which adjacent Cu(II) environments are related by 4_1 screw symmetry [13]. At zero field, the magnetism of $[Cu(pym)(H_2O)_4]SiF_6{\cdot}H_2O$ is well described by an $S = 1/2$ chain model and no long-range order is detected above 0.02 K, as evidenced by muon-spin relaxation measurements [14]. Single-crystal ESR shows the presence of staggered g-tensors, anisotropic staggered susceptibility and a rich low-temperature excitation spectrum. However, the low-temperature field-induced excitation gap observed in heat capacity is significantly suppressed compared to that of a traditional non-chiral staggered chain, and has an unexpected linear field dependence. We propose this is due to additional interactions arising from the four-fold periodic chiral structure. This study showcases how the ground state of a Q1D AF chain is modified when competing interactions are introduced and poses a challenge to theorists to develop new models to fully account for the data.

$[Cu(pym)(H_2O)_4]SiF_6{\cdot}H_2O$ crystallizes in chiral space group $P4_12_12$ [13]. Cu(II) ions are linked in chains by N—C—N moieties of pyrimidine, which propagate the intrachain exchange interactions (Fig. 1). The Cu coordination is a distorted octahedron consisting of CuN_2O_2 equatorial planes [Cu—N 2.009(4) and 2.000(4) Å, Cu—O 2.043(3) and 2.091(3) Å], and two O atoms in the axial positions [Cu—O 2.197(3) and 2.227(4) Å] [13] consistent with a Jahn-Teller elongation along this direction [15]. In this local symmetry, $g_\parallel > g_\perp$, where $g_\parallel$ is the g factor along the axial direction. Local environments of nearest-neighbor Cu ions within a chain, and hence their local g tensors, are related by a 90° rotation about the c-axis. Interchain sites are occupied by H_2O and SiF_6^{2-} anions, leading to a minimum interchain Cu—Cu dis-

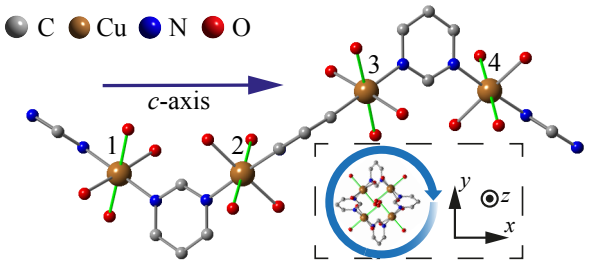

FIG. 1. Chain structure of $[Cu(pym)(H_20)_4]SiF_6{\cdot}H_2O$. H atoms and $[SiF_6]^{2-}$ counterions omitted for clarity. The unit cell houses four inequivalent Cu(II) ions. Staggered elongated Cu—O bonds (green) correspond to the local $g_\parallel$ axes. Inset: view along c-axis depicting four-fold rotation of the local environment about the chain direction.

tance of 7.480 Å.

Room temperature ESR measurements were performed at 240 GHz employing a quasi-optic setup to probe the g anisotropy. Representative spectra are shown in Fig. 2(a). A single resonance due to the strong interaction between Cu(II) ions is observed [11, 16]. The measured g factor is an average of the individual g tensors of the four magnetically inequivalent Cu(II) sites. The strong coupling between spins and the four-fold rotational symmetry ensure an isotropic ESR angle-dependence in the ab-plane, hence only two principal values, $g_{\max} = 2.21$ and $g_{\min} = 2.10$, can be extrapolated from ESR data [Fig. 2(b)] and to obtain the g values of the individual Cu(II) ions we must assume tetragonal local symmetry. Strictly the equatorial ligand pairs break this symmetry, but in other materials with similar Cu(II) environments for which the full g-tensor can be determined, it was found that $\Delta g_\perp = g_x - g_y$ is an order of magnitude smaller than $\Delta g = g_\parallel - g_\perp$ [17], mitigating the tetragonal approximation. We note that relaxing this assumption would have only a small effect on the size of the staggered fields discussed later. The principal g values of the individual Cu(II) ions are thus found to be $g_\parallel = 2.33$ and $g_\perp = 2.09$. These values are similar to those reported for Cu(II) ions in closely related local environments [11, 17]. In the xyz laboratory frame [14] the g tensor of the ith Cu(II) ion in a unit cell can be separated into three components:

$$\begin{aligned} g_i &= g_{\rm u} + g_{2s} + g_{4s} \\ &= \begin{pmatrix} 2.21 & 0 & 0 \\ 0 & 2.21 & 0 \\ 0 & 0 & 2.10 \end{pmatrix} + 0.12 \begin{pmatrix} 0 & (-1)^i & 0 \\ (-1)^i & 0 & 0 \\ 0 & 0 & 0 \end{pmatrix} \\ &+ 0.026 \begin{pmatrix} 0 & 0 & (-1)^i\delta_i \\ 0 & 0 & \delta_i \\ (-1)^i\delta_i & \delta_i & 0 \end{pmatrix} \end{aligned} \quad (1)$$

where δ_i = -1, +1, +1 and -1 respectively for i = 1, 2, 3 and 4 (see Fig. 1). $g_{\rm u}$ corresponds to the uniform part of the g-tensor, while g_{2s} is a small staggered component which repeats after every two nearest neighbour Cu(II) ions. g_{4s}, which we believe is so far unique to this material, is a much weaker staggered part with a four-fold period along the chain, i.e. the same periodicity as the unit cell. g_{2s} is similar in form and size to that seen in Cu-benzoate and $[pym\text{-}Cu(NO_3)_2(H_2O)_2]$ [7, 8, 11]. When a field H is applied perpendicular to the chain, g_{2s} will generate a staggered field that can open an excitation gap in the low-temperature spectrum.

Further variable frequency/temperature ESR measurements were performed in a broadband spectrometer. The temperature dependence of the spectra below 20 K are shown in Fig. 2(c). Upon cooling, the resonance shifts to lower field and eventually splits into two as indicated by arrows. Below 3 K, a series of resonances (marked by squares) quickly emerge at high field (above $g = 2$) with intensities that increase rapidly with lowering temperature, confirming the ground state nature of these excitations. The temperature and frequency [Fig. 2(d)] evolution of the lines cannot be explained by paramagnetic resonances of transition metals [18] or conventional antiferromagnetic resonances. In fact, the data are reminiscent of excitations observed in $[pym\text{-}Cu(NO_3)_2(H_2O)_2]$, where three branches were identified as breather modes of the SG model, along with six other modes more difficult to classify [12]. However, we find that the frequency-field dependence of our resonances *cannot* be modelled by the breather gaps proposed for SG chains [10, 12, 14].

Another important predicted feature due to staggered g-tensors is the existence of a low-temperature staggered susceptibility. Representative single-crystal susceptibility (χ) measurements performed down to 1.8 K are shown in the inset to Fig. 2(e). Above 10 K, the susceptibility can be well modelled as a uniform Heisenberg $S = 1/2$ chain [19] with AF exchange $J = 42.3 \pm 0.8$ K. This energy is consistent with the saturation field (≈ 65 T) observed in pulsed magnetic fields [14]. The value of J and lack of long-range order above 20 mK in zero field imply an upper limit of 7 mK on the size of the interchain coupling [20]. Below 10 K, an upturn in $\chi(T)$ emerges which can be described by an additional contribution proportional to $1/T$ and the entire temperature range can be fitted to $\chi(T) = \chi_{1D}(T) + \chi_s/T$ where $\chi_{1D}(T)$ is the Heisenberg chain contribution. The staggered susceptibility χ_s exhibits a pronounced angular dependence with its maximum value occurring when H is applied perpendicular to the chain. The strong anisotropy of χ_s confirms it is not due to paramagnetic impurities. Similar variation of χ_s is observed in Cu-benzoate [21] and $[pym\text{-}Cu(NO_3)_2(H_2O)_2]$ [11] and identified as an intrinsic property related to the staggered field [22].

Fig. 2(f) shows the magnetic contribution ($C_{\rm mag}$) to heat capacity for a deuterated sample of $[Cu(pym)(H_2O)_4]SiF_6{\cdot}H_2O$ down to 100 mK. A $C \sim T^{-2}$ low-temperature tail is subtracted from the data (except the zero-field data) to account for the

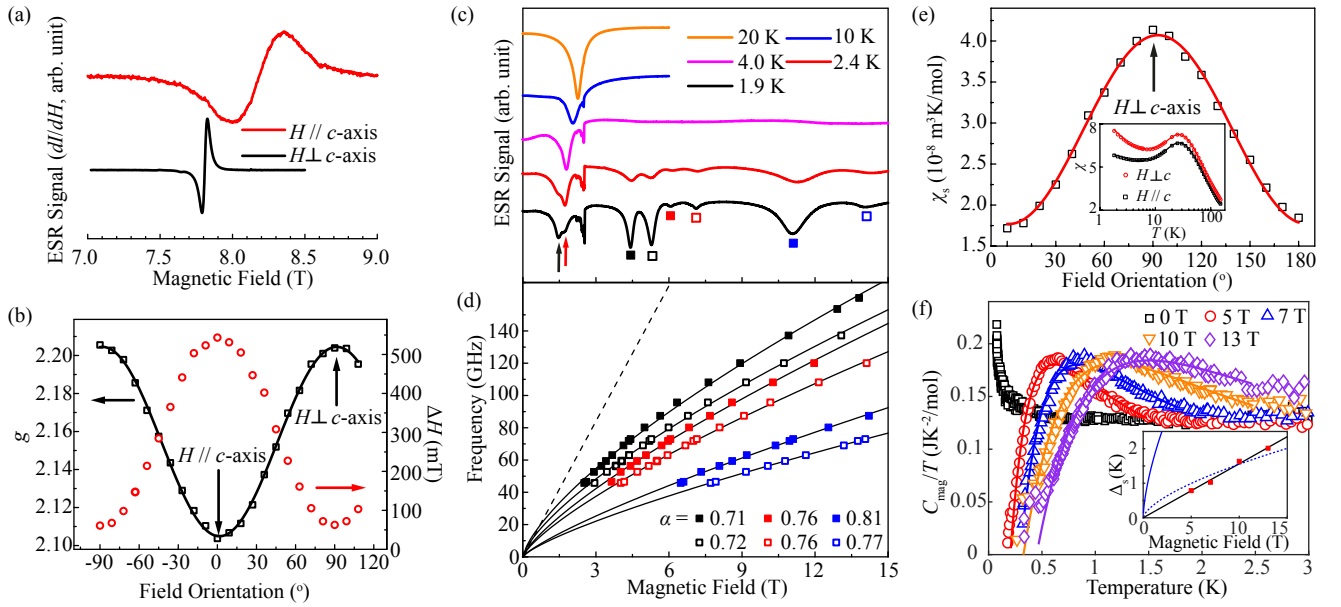

FIG. 2. (a) Room temperature ESR spectra at 240 GHz. A DM interaction and spin-diffusion could contribute to linewidth anisotropy [14]. (b) Orientation dependence of Cu(II) g factor (□) and linewidth (○) at 300 K. The line is a fit to $g(\theta) = (g_{\rm min}^2 \cos^2\theta + g_{\rm max}^2 \sin^2\theta)^{1/2}$. (c) and (d) ESR data with field $\perp c$. (c) Temperature dependence of ESR spectra at 73 GHz. (d) Frequency versus field (H) plot showing ESR peaks observed at 1.9 K using the labeling scheme in (c). Solid lines are fits to $f = AH^{\alpha}$ with α values shown. Dashed line is the paramagnetic resonance with $g = 2$. (e) Inset: representative χ vs. T data with $H = 0.2$ T. Solid line is the model $\chi(T) = \chi_{\rm 1D}(T) + \chi_{\rm s}/T$ described in the text. Main panel: angular variation of χ_s. The line is a fit to a $\cos^2$ dependence. (f) Temperature dependence of the magnetic contribution to heat capacity at different $H \perp c$. Lines are fits to a gapped model. Inset shows resulting field dependence of the gap (squares, size corresponds to largest y-axis error), a linear fit to the data (black line), the best fit to SG model (blue dotted line), and gap size predicted by SG model from experimental g_{2s} value (solid blue line).

nuclear contribution [14]. In zero field above 0.5 K, the nearly constant value of $C_{\rm mag}/T$ can be interpreted as the heat capacity of a uniform $S = 1/2$ AF Heisenberg chain in the TLL state, where $C_{\rm mag} = 2RT/3J$ [23, 24], giving $J = 41.9 \pm 1.5$ K in excellent agreement with the magnetometry data.

The field-induced gap in $[Cu(pym)(H_2O)_4]SiF_6{\cdot}H_2O$ is revealed by heat capacity measurements performed with $H \perp c$. On warming from low temperatures, $C_{\rm mag}$ is first suppressed below, and then rises above, the zero-field curve before meeting it at high temperature. This behaviour is identical to that of the non-chiral staggered chains [6, 11] and indicates the emergence of an excitation gap that increases with applied field. Given the similarities with the non-chiral staggered chains, the expression for the temperature dependence of $C_{\rm mag}$ derived from the SG model will provide the best possible estimate of the gap in our system at a particular magnetic field. However, fitting our data to the SG model [25] yields a gap of $\Delta_{\rm s} = 1.98$ K at 13 T, significantly smaller than the expected value of 8.24 K, calculated using g_{2s} and J values obtained from ESR and magnetometry. More importantly, the field evolution of the gap exhibits $\Delta_{\rm s} \propto H$ [inset to Fig. 2(f)], which is distinctly different from the expectation of the SG model, where $\Delta_{\rm s} \propto H^{2/3}$ [7].

It is clear that $[Cu(pym)(H_2O)_4]SiF_6{\cdot}H_2O$ exhibits the staggered g-tensors, ground-state excitations and field-induced spin gap similar to those seen in the SG chains. However, the size of the gap and its linear field dependence are inconsistent with theoretical predictions for a traditional staggered system. We believe that we can qualitatively account for the departures from the existing theories based on differences between the chiral and non-chiral staggered structures.

The staggered fields in the existing model of Cu-benzoate are compared to our chiral chain in Fig. 3. In both cases the chains lie along $\mathbf{Z}$ and the applied field $\mathbf{H}_0 \parallel \mathbf{X}$. For Cu-benzoate, a canted spin configuration, caused by competition between AF exchange and H_0, is stabilized in the XZ-plane by the same two-fold periodic staggered fields $\mathbf{h}_{2s} \| \mathbf{Z}$ that are responsible for the gap [8]. In contrast in the chiral system, the measured g-tensor (Eq. 1) gives rise to two-fold staggered fields perpendicular to both $\mathbf{H}_0$ and $\mathbf{Z}$. Thus if the spins adopt a canting in the XZ plane, the coupling to $\mathbf{h}_{2s} \| \mathbf{Y}$ will be lost. This would be a simple explanation for the observed suppression of the field-induced gap, but requires an additional interaction, not present in previously studied staggered

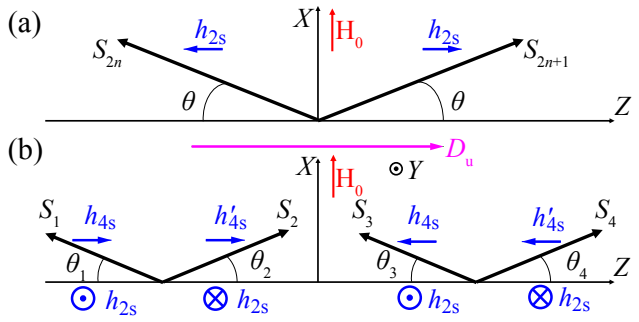

FIG. 3. Classical spin configurations for the unit cell of (a) Cu-benzoate and (b) $[Cu(pym)(H_2O)_4]SiF_6{\cdot}H_2O$ in applied field $H_0 \parallel X$-axis. Z is the chain direction. Also shown are relative directions of the two-fold and four-fold staggered fields (h_{2s}, h_{4s} and h'_{4s}), and uniform DM interaction (D_u) allowed in $[Cu(pym)(H_2O)_4]SiF_6{\cdot}H_2O$. The XZ canting in (b) would minimize coupling between the spins and h_{2s}.

chains, that would favor XZ over XY canting. The crystal symmetry of $[Cu(pym)(H_2O)_4]SiF_6{\cdot}H_2O$ permits such an interaction in the form of an equal and opposite DM interaction on nearest-neighbor chains. By symmetry, the DM interaction of a given chain can be decomposed into a uniform component parallel to the chain axis of magnitude D_u, and a four-fold periodic staggered component perpendicular to the chain axis. Including the uniform DM term and applying $\mathbf{H}_0 \parallel \mathbf{X}$, the Hamiltonian can be written as,

$$\begin{aligned}\hat{\mathcal{H}} = &\sum_i J(\hat{S}_i^X \hat{S}_{i+1}^X + \hat{S}_i^Y \hat{S}_{i+1}^Y + \lambda \hat{S}_i^Z \hat{S}_{i+1}^Z) \\ &+ \sum_i D_u(\hat{S}_i^X \hat{S}_{i+1}^Y - \hat{S}_i^Y \hat{S}_{i+1}^X) + \sum_i H_0 g_u \hat{S}_i^X \\ &+ \sum_i g_{2s} H_0 \hat{S}_i^Y + \sum_i g_{4s} H_0 \hat{S}_i^Z,\end{aligned} \tag{2}$$

where J is the intrachain AF exchange, which can now possess a small anisotropy ($\lambda \approx 1$).

The classical model of an $S = 1/2$ chain with uniform g_u and D_u in a transverse H_0 predicts an incommensurate-commensurate transition at $H_0 = \pi D_u S$, where the ground state at high fields is an AF canted structure lying in the XY or XZ plane for $\lambda < 1$ or $\lambda > 1$, respectively. Recent quantum analyses of the same model shows that XZ canting is preferred for a substantial field range, even with a weak easy-plane type exchange anisotropy ($\lambda < 1$) [26, 27]. In our case this would effectively mitigate the effect of the small two-fold staggered field along Y. At low magnetic fields, the ground state of the model is an incommensurate helical XY antiferromagnet with propagation vector along $\mathbf{Z}$ [26–28]. Averaged across the chain, this structure will also negate the effect of the h_{2s} term, which is commensurate, resulting in a reduced gap. Furthermore, the quantum simulations show that a tiny field component parallel to the chain, e.g. caused by experimental sample misalignment, will stabilize the gapless XY helical phase against a strong transverse field [26], allowing the XY canted phase that couples strongly to h_{2s} to appear only in the presence of a considerable easy-plane anisotropy. Hence, we expect the ground state to show either an XY helix or XZ canting (or a mixture). In either case, the coupling to h_{2s} will be significantly weakened compared to the staggered chains considered previously, leading to suppression of the field-induced gap.

An interesting consequence of the chiral crystal structure with XZ spin-canting is that while $\mathbf{h}_{2s}$ is perpendicular to the spins, the weaker staggered fields $\mathbf{h}_{4s} = g_{4s}\mathbf{H}_0$ are parallel to $\mathbf{Z}$ [Fig. 3(b)] and so contribute to the excitation spectrum potentially producing a field-induced gap. To explore this, we consider a spin-wave model of an $S = 1/2$ Heisenberg chain in the XZ canted configuration with mutually perpendicular uniform and staggered fields. As noted earlier, in principle $g_x \neq g_y$, meaning that h_{4s} acting on neighbouring ions need not be identical. Nevertheless, the space group symmetry of $[Cu(pym)(H_2O)_4]SiF_6{\cdot}H_2O$ requires that: (i) these staggered fields have a four-fold repetition; and (ii) next-nearest neighbors within a chain, which are related by a 180° rotation, must experience equal, but opposite values. This is different to the staggered fields that open the gap in Cu-benzoate, where $\mathbf{h}_{2s}$ takes opposite values on adjacent sites [Fig. 3(a)]. In both cases, the exchange interaction ensures that the magnetic moment along the chain is antiparallel for neighboring ions. The first order spin-wave approximation suggests that the spin-canting angle only depends on the external field $H_0 \gg h_{4s}$ and the interaction J, specifically $\theta_i = \theta = \sin^{-1}(H_0/4JS)$ for all spins. Thus the classical energy contribution of the four-fold staggered field is:

$$E_{4s} = \cos\theta(h_{4s}S - h'_{4s}S - h_{4s}S + h'_{4s}S) = 0, \tag{3}$$

where h_{4s} and h'_{4s} are the staggered-field values on odd and even sites, respectively. This complete cancellation implies that to first order in the spin-wave approximation, the four-fold staggered field in $[Cu(pym)(H_2O)_4]SiF_6{\cdot}H_2O$ has no contribution to its energy spectrum, whereas in Cu-benzoate the field-induced gap is readily seen in the first-order perturbation [7]. Only when the analysis is extended to second order by considering the corrections to the canting angles θ_j due to $\mathbf{h}_{4s}$ and $\mathbf{h}'_{4s}$ will a gap start to emerge [14].

Summarizing, we propose the key differences between the nature of the gap observed in chiral $[Cu(pym)(H_2O)_4]SiF_6{\cdot}H_2O$ and the traditional staggered chains reside in a low-temperature spin configuration that decouples the system, fully or partially, from the two-fold staggered field, and is favored by the presence of a uniform DM interaction. In the event of a mixture of XY, XZ or helical configurations, the effect of h_{2s} on the excitation spectrum is still important, but will be altered

from existing models. In addition, and particularly for the situation of complete decoupling of the spins from h_{2s}, the added presence of the four-fold staggered field necessitates new theoretical predictions for the size and field-dependence of the gap, as well as for the excitation modes seen in ESR. We note it is possible that in applied field the XZ canted phase itself could exhibit a gap in the absence of staggered fields [29].

The purely XZ canting shown in Fig. 3(b) relies on the uniform DM interaction being significantly stronger than h_{2s}. We expect $D_u \propto (\Delta g/g)J \gg h_{2s}$ for the experimental field range, and the smooth linear evolution of the gap up to 13 T [inset to Fig. 2(f)] suggests no abrupt spin orientation takes place, however the data do not permit an unambiguous estimate of D_u. We point out again that a staggered DM interaction is allowed by the symmetry of $[Cu(pym)(H_2O)_4]SiF_6{\cdot}H_2O$ and must be considered in any future theoretical model.

Our results demonstrate that spin chains in which local magnetic environments are related via screw symmetry can present a remarkable suppression of the field-induced SG spin gap via emergence of uniform DM interactions and complex staggered fields. This opens up the possibility of searching for other materials where anisotropic interactions and particular crystal symmetries conspire to enable entirely novel magnetic states.

We thank EPSRC for support. PAG acknowledges that this project has received funding from the European Research Council (ERC) under the European Union's Horizon 2020 research and innovation programme (grant agreement No. 681260). RDJ acknowledges financial support from the Royal Society. A portion of this work was performed at the National High Magnetic Field Laboratory, which is supported by National Science Foundation Cooperative Agreement No. DMR-1157490 and the State of Florida, as well as the *Strongly Correlated Magnets* thrust of the DoE BES "Science in 100 T" program. The work at EWU was supported by the NSF through grant no. DMR-1703003. We are grateful for the provision of beam time for muon measurements at the STFC ISIS Facility, UK and the Swiss Muon Source, Paul Scherrer Institut, Switzerland, and to F.L. Pratt and C. Baines for experimental assistance. Roberts Williams is thanked for useful discussions. Data presented in this paper resulting from the UK effort will be made available at XXXXXXX.

* jmanson@ewu.edu
† p.goddard@warwick.ac.uk

[1] M. Hagiwara, H. Tsujii, C. R. Rotundu, B. Andraka, Y. Takano, N. Tateiwa, T. C. Kobayashi, T. Suzuki, and S. Suga, Phys. Rev. Lett. **96**, 147203 (2006).
[2] C. Rüegg, K. Kiefer, B. Thielemann, D. F. McMorrow, V. Zapf, B. Normand, M. B. Zvonarev, P. Bouillot, C. Kollath, T. Giamarchi, S. Capponi, D. Poilblanc, D. Biner, and K. W. Krämer, Phys. Rev. Lett. **101**, 247202 (2008).
[3] M. Klanjšek, H. Mayaffre, C. Berthier, M. Horvatić, B. Chiari, O. Piovesana, P. Bouillot, C. Kollath, E. Orignac, R. Citro, and T. Giamarchi, Phys. Rev. Lett. **101**, 137207 (2008).
[4] M. Jeong, H. Mayaffre, C. Berthier, D. Schmidiger, A. Zheludev, and M. Horvatić, Phys. Rev. Lett. **111**, 106404 (2013).
[5] T. Giamarchi, *Quantum Physics in One Dimension* (Oxford University Press, Oxford, 2004).
[6] D. C. Dender, P. R. Hammar, D. H. Reich, C. Broholm, and G. Aeppli, Phys. Rev. Lett. **79**, 1750 (1997).
[7] M. Oshikawa and I. Affleck, Phys. Rev. Lett. **79**, 2883 (1997).
[8] I. Affleck and M. Oshikawa, Phys. Rev. B **60**, 1038 (1999).
[9] F. H. L. Essler and A. M. Tsvelik, Phys. Rev. B **57**, 10592 (1998).
[10] F. H. L. Essler, A. Furusaki, and T. Hikihara, Phys. Rev. B **68**, 064410 (2003).
[11] R. Feyerherm, S. Abens, D. Günther, T. Ishida, M. Meißner, M. Meschke, T. Nogami, and M. Steiner, J. Phys.: Condens. Matter **12**, 8495 (2000).
[12] S. A. Zvyagin, A. K. Kolezhuk, J. Krzystek, and R. Feyerherm, Phys. Rev. Lett. **93**, 027201 (2004).
[13] D. B. Cordes, C. V. Krishnamohan Sharma, and R. D. Rogers, Cryst. Growth Des. **7**, 1943 (2007).
[14] See Supplemental Material at http://link.aps.org/ for detailed information on methods, calculations and ancillary experiments, including Refs. [30–41].
[15] R. J. Deeth and M. A. Hitchman, Inorganic Chemistry **25**, 1225 (1986).
[16] P. W. Anderson, J. Phys. Soc. Jpn. **9**, 316 (1954).
[17] J. L. Manson, M. M. Conner, J. A. Schlueter, A. C. McConnell, H. I. Southerland, I. Malfant, T. Lancaster, S. J. Blundell, M. L. Brooks, F. L. Pratt, J. Singleton, R. D. McDonald, C. Lee, and M.-H. Whangbo, Chemistry of Materials **20**, 7408 (2008).
[18] J. Krzystek, A. Ozarowski, and J. Telser, Coordination Chemistry Reviews **250**, 2308 (2006).
[19] D. C. Johnston, R. K. Kremer, M. Troyer, X. Wang, A. Klümper, S. L. Bud'ko, A. F. Panchula, and P. C. Canfield, Phys. Rev. B **61**, 9558 (2000).
[20] C. Yasuda, S. Todo, K. Hukushima, F. Alet, M. Keller, M. Troyer, and H. Takayama, Phys. Rev. Lett. **94**, 217201 (2005).
[21] M. Date, H. Yamazaki, M. Motokawa, and S. Tazawa, Supplement of the Progress of Theoretical Physics **46**, 194 (1970).
[22] S. Glocke, A. Klümper, H. Rakoto, J. M. Broto, A. U. B. Wolter, and S. Süllow, Phys. Rev. B **73**, 220403 (2006).
[23] I. Affleck, Phys. Rev. Lett. **56**, 746 (1986).
[24] T. Xiang, Phys. Rev. B **58**, 9142 (1998).
[25] F. H. L. Eßler, Phys. Rev. B **59**, 14376 (1999).
[26] I. Garate and I. Affleck, Phys. Rev. B **81**, 144419 (2010).
[27] Y. H. Chan, W. Jin, H. C. Jiang, and O. A. Starykh, Phys. Rev. B **96**, 1 (2017).
[28] D. N. Aristov and S. V. Maleyev, Phys. Rev. B **62**, R751 (2000).
[29] S. Gangadharaiah, J. Sun, and O. A. Starykh, Phys. Rev. B **78**, 054436 (2008), see page 13.
[30] S. J. Blundell, Contemporary Physics **40**, 175 (1999),

0207699.
[31] R. S. Hayano, Y. J. Uemura, J. Imazato, N. Nishida, T. Yamazaki, and R. Kubo, Physical Review B **20**, 850 (1979).
[32] T. G. Castner and M. S. Seehra, Physical Review B **4**, 38 (1971).
[33] A. Zorko, D. Arčon, H. van Tol, L. C. Brunel, and H. Kageyama, Physical Review B **69**, 174420 (2004).
[34] M. Herak, A. Zorko, D. Arčon, A. Potočnik, M. Klanjšek, J. van Tol, A. Ozarowski, and H. Berger, Physical Review B **84**, 184436 (2011), 1109.5597.
[35] S. J. Balian, G. Wolfowicz, J. J. L. Morton, and T. S. Monteiro, Phys. Rev. B **89**, 045403 (2014).
[36] M. Shiddiq, D. Komijani, Y. Duan, A. Gaita-Ario, E. Coronado, and S. Hill, Nature **531**, 348 (2016).
[37] K. Y. Povarov, A. I. Smirnov, O. A. Starykh, S. V. Petrov, and A. Y. Shapiro, Phys. Rev. Lett. **107**, 037204 (2011).
[38] A. I. Smirnov, T. A. Soldatov, K. Y. Povarov, M. Hälg, W. E. A. Lorenz, and A. Zheludev, Phys. Rev. B **92**, 134417 (2015).
[39] S. A. Zvyagin, Low Temperature Physics **38**, 819 (2012).
[40] K. An, T. Sakakibara, R. Settai, Y. Onuki, M. Hiragi, M. Ichioka, and K. Machida, Physical Review Letters **104**, 1 (2010), 0911.3443.
[41] P. A. Goddard, J. Singleton, P. Sengupta, R. D. McDonald, T. Lancaster, S. J. Blundell, F. L. Pratt, S. Cox, N. Harrison, J. L. Manson, H. I. Southerland, and J. A. Schlueter, New Journal of Physics **10**, 083025 (2008).